

Theoretical Study of Silylene Substituent Effects on the Abstraction Reactions with Oxirane and Thiirane

Ming-Der Su*

Contribution from the School of Chemistry, Kaohsiung Medical University,
Kaohsiung 80708, Taiwan, R.O.C.

Received April 8, 2002

Abstract: The potential energy surfaces for the abstraction reactions of silylenes with oxirane and thiirane have been characterized in detail using density functional theory (B3LYP) as well as the ab initio method (QCISD), including zero-point corrections. Five silylene species including SiH_2 , $\text{Si}(\text{CH}_3)_2$, $\text{Si}(\text{NH}_2)_2$, $\text{Si}(\text{OH})_2$, and SiF_2 have been chosen in this work as model reactants. All the interactions involve the initial formation of a donor–acceptor ylide-like complex followed by a heteroatom shift via a two-center transition state. The complexation energies, activation barriers, and enthalpies of the reactions were used comparatively to determine the relative silylenic reactivity, as well as the influence of substituents on the reaction potential energy surface. As a result, our theoretical investigations suggest that, irrespective of deoxygenation and desulfurization, the alkyl-substituted silylene abstractions are much more favorable than those of the π donor-substituted silylenes. Moreover, for a given silylene, while both deoxygenation and desulfurization are facile processes, the deoxygenation reaction is more exothermic as well as more kinetically favorable. Furthermore, a configuration mixing model based on the work of Pross and Shaik is used to rationalize the computational results. The results obtained allow a number of predictions to be made.

I. Introduction

Silylenes (SiR_2), the silicon analogues of carbenes in organic chemistry, are key intermediates in many thermal and photochemical reactions of organosilicon compounds and have, therefore, been extensively studied both experimentally and theoretically.^{1–3} A diverse set of silylenes is known,⁴ and they display high reactivities toward a variety of organic compounds.^{1–3} In fact, in recent years, the main emphasis has focused on studies of their reactivities and synthetic use⁵ as well as on the search for stable silylenes.⁶

In principle, once formed, silylenes can react by insertion, dimerization, disproportionation, and cycloaddition.^{1,2,7} Similar processes exist for carbenes as well.⁸ Nevertheless, to the best of our knowledge, until now, neither experimental nor theoretical work has been devoted to the study of the deoxygenation of organic compounds by silylenes, let alone a systematic study of the effects of substituents on the reactivities of silylene species. Besides this, reductive desulfurization of organic molecules by silylenes, whose chemistry parallels that of deoxygenation, has not yet been established by either experimental or theoretical studies, and many key questions remain open. It is astonishing how little is known about the abstraction reactions of silylenes, considering their importance in synthetic organosilicon chemistry^{1–3} and the extensive research activity on the corresponding carbene species.^{9–11}

It is these unsolved problems that arouse our interest. The object of this study is, thus, to reach a more thorough understanding of silylene chemistry. To this end, we have now

* To whom correspondence should be addressed. E-mail: midesu@cc.kmu.edu.tw.

- (1) For the most recent reviews, see: (a) Okazaki, R.; Tokitoh, N. *Acc. Chem. Res.* **2000**, *33*, 625. (b) Tokitoh, N.; Matsumoto, T.; Okazaki, R. *Bull. Chem. Soc. Jpn.* **1999**, *72*, 1665. (c) Auner, N.; Weis, J. In *Organosilicon Chemistry*; VCH: Weinheim, Germany, 1994. (d) Auner, N.; Weis, J. In *Organosilicon Chemistry II*; VCH: Weinheim, Germany, 1996. (e) Auner, N.; Weis, J. In *Organosilicon Chemistry III*; VCH: Weinheim, Germany, 1998. (f) Auner, N.; Weis, J. In *Organosilicon Chemistry IV*; VCH: Weinheim, Germany, 2000.
- (2) (a) Gaspar, P. P. In *Reactive Intermediates*; Jones, M., Jr., Moss, R. A., Eds.; Wiley: New York, 1981; Vol. 2, pp 335–385. (b) Gaspar, P. P. In *Reactive Intermediates*; Jones, M., Jr., Moss, R. A., Eds.; Wiley: New York, 1985; Vol. 3, pp 333–427.
- (3) Jasinski, J. M.; Meyerson, B. S.; Scott, B. A. *Annu. Rev. Phys. Chem.* **1987**, *38*, 109.
- (4) (a) Margrave, J. L.; Wilson, P. W. *Acc. Chem. Res.* **1971**, *4*, 145. (b) Lee, H. U.; DeNeufville, J. P. *Chem. Phys. Lett.* **1983**, *99*, 394. (c) Dubois, I. *Can. J. Phys.* **1968**, *46*, 2485. (d) Rao, V. M.; Curl, R. F.; Timms, P. L.; Margrave, J. L. *J. Chem. Phys.* **1965**, *43*, 2557. (e) Milligan, D. E.; Jacox, M. E. *J. Chem. Phys.* **1970**, *52*, 2594. (f) Ismail, Z. K.; Fredin, L.; Hauge, R. H.; Margrave, J. L. *J. Chem. Phys.* **1982**, *77*, 1626.
- (5) (a) Chernyshev, E. A.; Komalenkova, N. G. *Sov. Sci. Rev., Sect. B* **1994**, *12*, 107. (b) Weidenbruch, M. *Coord. Chem. Rev.* **1994**, *130*, 275.
- (6) (a) Denk, M.; Lennon, R.; Hayashi, R.; West, R.; Belyakov, A. V.; Verne, H. P.; Haaland, A.; Wagner, M.; Metzler, N. *J. Am. Chem. Soc.* **1994**, *116*, 2691. (b) Denk, M.; West, R.; Hayashi, R.; Apeloig, Y.; Pauncz, R.; Karni, M. In *Organosilicon Chemistry II*; Auner, N., Weis, J., Eds.; VCH: New York, 1996; pp 251–261.
- (7) (a) West, R.; Barton, T. J. *J. Chem. Educ.* **1980**, *57*, 165. (b) West, R.; Barton, T. J. *J. Chem. Educ.* **1980**, *57*, 335.
- (8) (a) Kirmse, W. *Carbene Chemistry*, 2nd ed.; Academic Press: New York, 1971. (b) Moss, R. A.; Jones, M., Jr. *Carbenes*; Wiley: New York, 1973; Vol. 1. (c) Jones, M., Jr.; Moss, R. A. *Carbenes*; Wiley: New York, 1975; Vol. 2. (d) Moss, R. A.; Jones, M., Jr. *Reactive Intermediates*; Wiley: New York, 1978; Vol. 1. (e) Moss, R. A.; Jones, M., Jr. *Reactive Intermediates*; Wiley: New York, 1981; Vol. 2. (f) Moss, R. A.; Jones, M., Jr. *Reactive Intermediates*; Wiley: New York, 1985; Vol. 3. (g) Abramovitch, R. A. *Reactive Intermediates*; Plenum: New York, 1980; Vol. 1.
- (9) (a) Pezacki, J. P.; Wood, P. D.; Gadosy, T. A.; Lusztzyk, J.; Warkentin, J. *J. Am. Chem. Soc.* **1998**, *120*, 8681. (b) Wittig, G.; Schlosser, M. *Tetrahedron* **1962**, *18*, 1026. (c) Nozaki, H.; Takaya, H.; Noyori, R. *Tetrahedron Lett.* **1965**, 2563. (d) Nozaki, H.; Takaya, H.; Noyori, R. *Tetrahedron* **1966**, *22*, 3393. (e) Martin, M. G.; Ganem, B. *Tetrahedron Lett.* **1984**, 251. (f) Shields, C. J.; Schuster, G. B. *Tetrahedron Lett.* **1987**, *28*, 853.

undertaken a systematic investigation of the abstraction reactions of several symmetrically substituted silylenes, SiH_2 , $\text{Si}(\text{CH}_3)_2$, $\text{Si}(\text{NH}_2)_2$, $\text{Si}(\text{OH})_2$, and SiF_2 , with oxirane and thiirane by using the density functional theory (DFT). With this theoretical study, we hope (i) to obtain a detailed understanding of the reactivities of a variety of silylenes toward oxirane and thiirane, (ii) to investigate the influence of different substituted groups upon the geometries and energies of both the intermediates and the transition states, (iii) to predict the trends in activation energies and reaction enthalpies, (iv) to probe electronic effects on the reactivities in a series of disubstituted silylenes, and (v) to highlight the factors that can facilitate both oxirane deoxygenation and thiirane desulfurization, which may suggest further synthetic applications.

II. Theoretical Methods

All geometries were fully optimized without imposing any symmetry constraints, although, in some instances, the resulting structure showed various elements of symmetry. For our DFT calculations, we used the hybrid gradient-corrected exchange functional proposed by Becke,¹² combined with the gradient-corrected correlation functional of Lee, Yang, and Parr.¹³ This functional is commonly known as B3LYP and has been shown to be quite reliable for computing geometries.¹⁴ A standardized 6-311G basis set¹⁵ was used together with polarization (d) functions.¹⁶ We denote our B3LYP calculations by B3LYP/6-311G(d). The spin-unrestricted (UB3LYP) formalism used for the open-shell (triplet) species and their $\langle S^2 \rangle$ values were nearly all equal to the ideal value (2.00). Vibrational frequency calculations at the B3LYP/6-311G(d) level were used to characterize all stationary points as either minima (the number of imaginary frequencies (NIMAG) = 0) or transition states (NIMAG = 1). The relative energies are, thus, corrected for vibrational zero-point energies (ZPE, not scaled).

For better energetics, single-point calculations were made at the QCISD level¹⁷ using the 6-311+G(2d,p) basis set. Unless otherwise noted, the relative energies given in the text are those determined at QCISD/6-311+G(2d,p)/B3LYP/6-311G(d) (hereafter designed QCISD) and include vibrational ZPE (without scale) corrections determined at B3LYP/6-311G(d). All of the DFT and QCISD calculations were performed with the GAUSSIAN94 package of programs.¹⁸

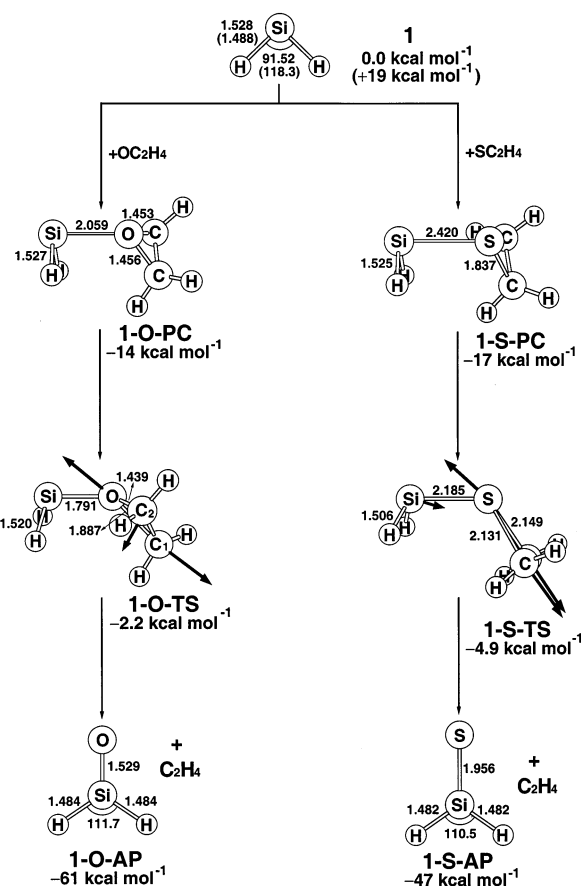


Figure 1. B3LYP/6-311G(d) geometries (in Å and deg) for the precursor complexes (PC), transition states (TS), and abstraction products (AP) of oxirane with SiH_2 (**1**). The relative energies were obtained at the QCISD level of theory. Values in parentheses are in the triplet state. The heavy arrows indicate the main atomic motions in the transition state eigenvector.

III. Results and Discussion

A. Reactants. It is well established that silylene has a relatively low-lying σ lone-pair orbital and a higher-lying π (p in Si) orbital.¹⁹ The dominant configuration of a singlet silylene is $\sigma^2\pi^0$, while that of a triplet is $\sigma^1\pi^1$. The optimized reactant geometries (Rea), that is, SiH_2 (**1**), $\text{Si}(\text{CH}_3)_2$ (**2**), $\text{Si}(\text{NH}_2)_2$ (**3**), $\text{Si}(\text{OH})_2$ (**4**), and SiF_2 (**5**), for each reaction obtained at the B3LYP/6-311G(d) level of theory are collected in Figures 1–5, respectively. The triplet structures of these silylenes (**1**–**5**) were also optimized (UB3LYP/6-311G(d)), and their geometrical parameters are shown in parentheses. Calculated values for the energy difference ΔE_{st} ($= E_{\text{triplet}} - E_{\text{singlet}}$) between the singlet and triplet states of various silylenes are given in Table 1; a positive value for ΔE_{st} implies that the singlet is predicted to be the ground state rather than the triplet.

As is usually the case in group 14 divalent compounds, the triplet state has significantly wider bond angles ($\angle\text{XSiX}$) and shorter bond distances (Si–X) than the closed-shell singlet state.²⁰ There are, however, three exceptions found in $\text{Si}(\text{NH}_2)_2$, $\text{Si}(\text{OH})_2$, and SiF_2 , in which the optimum Si–X (X = NH_2 ,

- (10) Recently, through the elegant studies performed by Luszyk, Warkentin, and many co-workers,^{9a} it was found that singlet carbenes are capable of abstracting an oxygen atom from oxirane as well as a sulfur atom from thiirane. Several qualitative conclusions concerning the oxirane deoxygenation were obtained. (1) The magnitudes of the rate constants for oxygen atom transfer are dependent on the philicity of the carbene intermediate. (2) Trends in the kinetic data suggest that oxygen atom transfer occurs by a concerted mechanism through ylide-like transition states. (3) Ylides formed by the attack of carbenes on heteroatom donors were not actually observed for any of the heteroatom transfer reactions. (4) Absolute rate constants for the heteroatom transfer show that oxirane deoxygenation is a facile process.
- (11) (a) Su, M.-D.; Chu, S.-Y. *Chem.—Eur. J.* **2000**, *6*, 3777. (b) Su, M.-D.; Chu, S.-Y. *Chem. Phys. Lett.* **2000**, *320*, 475.
- (12) (a) Becke, A. D. *Phys. Rev. A* **1988**, *38*, 3098. (b) Becke, A. D. *J. Chem. Phys.* **1993**, *98*, 5648.
- (13) (a) Lee, C.; Yang, W.; Parr, R. G. *Phys. Rev. B* **1988**, *37*, 785. (b) Miehlich, B.; Savin, A.; Stoll, H.; Preuss, H. *Chem. Phys. Lett.* **1989**, *157*, 200.
- (14) (a) Jursic, B.; Zdravkovski, Z. *J. Chem. Soc., Perkin Trans.* **1995**, 1223. (b) Jursic, B. *Chem. Phys. Lett.* **1996**, *256*, 603. (c) Jursic, B. *THEOCHEM* **1998**, *425*, 193. (d) Jursic, B. *THEOCHEM* **1998**, *452*, 145.
- (15) Krishnan, R.; Binkley, J. S.; Pople, J. A. *J. Chem. Phys.* **1980**, *72*, 650.
- (16) McLean, A. D.; Chandler, G. S. *J. Chem. Phys.* **1980**, *72*, 5639.
- (17) Pople, J. A.; Head-Gordon, M.; Raghavachari, K. *J. Chem. Phys.* **1987**, *87*, 5968.
- (18) Frisch, M. J.; Trucks, G. W.; Schlegel, H. B.; Gill, P. M. W.; Johnson, B. G.; Robb, M. A.; Cheeseman, J. R.; Keith, T.; Peterson, G. A.; Montgomery, J. A.; Raghavachari, K.; Al-Laham, M. A.; Zakrzewski, V. G.; Ortiz, J. V.; Foresman, J. B.; Cioslowski, J.; Stefanov, B. B.; Nanayakara, A.; Challacombe, M.; Peng, C. Y.; Ayala, P. Y.; Chen, W.; Wong, M. W.; Andres, J. L.; Replogle, E. S.; Gomperts, R.; Martin, R. L.; Fox, D. J.; Binkley, J. S.; Defrees, D. J.; Baker, J.; Stewart, J. P.; Head-Gordon, M.; Gonzalez, C.; Pople, J. A. *GAUSSIAN94*; Gaussian, Inc.: Pittsburgh, PA, 1995.

- (19) (a) Berkowitz, J. L.; Greene, P. R.; Cho, H.; Ruscic, R. *J. Chem. Phys.* **1987**, *86*, 1235. (b) Bauschlicher, C. W.; Taylor, P. R. *J. Chem. Phys.* **1987**, *86*, 1420. (c) Balasubramian, K.; McLean, A. D. *J. Chem. Phys.* **1986**, *85*, 5117. (d) Charles, W.; Bauschlicher, Jr.; Langhoff, S. R.; Taylor, P. R. *J. Chem. Phys.* **1987**, *87*, 387.
- (20) (a) Mueller, P. H.; Rondan, N. G.; Houk, K. N.; Harrison, J. F.; Hooper, D.; Willen, B. H.; Leibman, J. F. *J. Am. Chem. Soc.* **1981**, *103*, 5049. (b) Carter, E. A.; Goddard, W. A., III. *J. Chem. Phys.* **1988**, *88*, 1752.

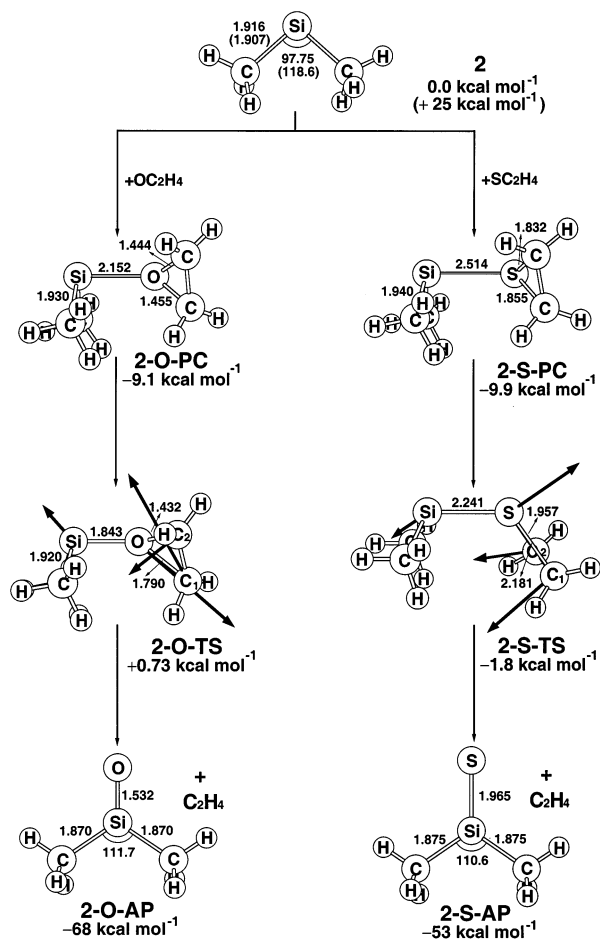


Figure 2. B3LYP/6-311G(d) geometries (in Å and deg) for the precursor complexes (PC), transition states (TS), and abstraction products (AP) of oxirane with $\text{Si}(\text{CH}_3)_2$ (**2**). The relative energies were obtained at the QCISD level of theory. Values in parentheses are in the triplet state. The heavy arrows indicate the main atomic motions in the transition state eigenvector.

OH, and F) bond lengths in the triplets are longer than those in the singlet states. The reason for this is presumably due to the fact that conjugation of the triplet silylene π electron to the two π electrons of the π -donor group is less important than the delocalization of the latter into the empty p - π orbital on the silylene silicon atom in the singlet state.

A key quantity, which has proved to be difficult to determine experimentally for silylenes, is the energy separation between the lowest singlet (1A_1) and triplet (3B_1) states. Several extensive reviews of theoretical and experimental results for SiH_2 are available.¹⁹ Recently, Berkowitz and co-workers have measured the singlet–triplet splitting value in SiH_2 as either $21.0 (\pm 0.7)$ or $18.0 (\pm 0.7)$.^{19a} This value is in good agreement with the present calculation, which gives 18.7 kcal/mol at QCISD/6-311+G(2d,p)//B3LYP/6-311G(d) level of theory. In fact, because of the difficulty of observing singlet–triplet electronic transitions directly, very few silylene singlet–triplet splitting values are known. One exception appears to be SiF_2 , for which the spectroscopic value of 75.2 kcal/mol has been reported.²¹ Our theoretical predictions of the singlet–triplet separation for SiF_2 are 74.8 and 71.8 kcal/mol at B3LYP and QCISD levels, respectively, which are in close agreement with experimental values.

(21) Rao, D. R. *J. Mol. Spectrosc.* **1970**, *34*, 284.

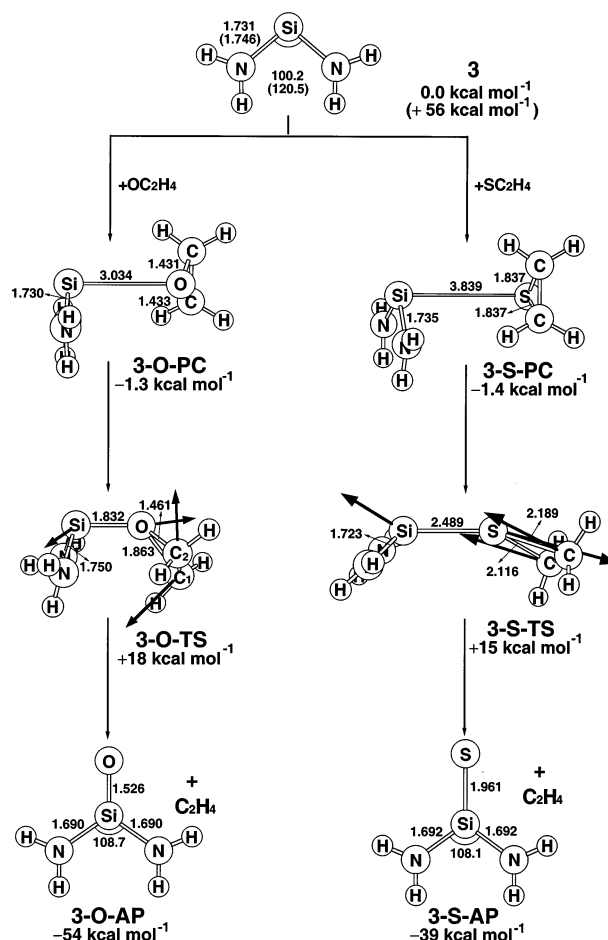


Figure 3. B3LYP/6-311G(d) geometries (in Å and deg) for the precursor complexes (PC), transition states (TS), and abstraction products (AP) of oxirane with $\text{Si}(\text{NH}_2)_2$ (**3**). The relative energies were obtained at the QCISD level of theory. Values in parentheses are in the triplet state. The heavy arrows indicate the main atomic motions in the transition state eigenvector.

Moreover, our calculations indicate that all the above silylene species (**1–5**) should have a singlet ground state. Indeed, to date, all known silylene SiR_2 species possess a singlet ground state without any experimentally verified exception.²² From Table 1, it is intriguing to find that their singlet–triplet energy splitting increases as the substituent changes across the periodic table from C to F. Namely, the stability of the singlet state of a substituted silylene relative to its triplet state increases with the electronegativity of the substituent. For example, the singlet–triplet energy splittings (QCISD) increase in the order: SiH_2 (19 kcal/mol) < $\text{Si}(\text{CH}_3)_2$ (25 kcal/mol) < $\text{Si}(\text{NH}_2)_2$ (56 kcal/mol) < $\text{Si}(\text{OH})_2$ (62 kcal/mol) < SiF_2 (72 kcal/mol). We shall use the above results to explain the origin of barrier heights for abstraction reactions in a later section.

On the other hand, the optimized geometries of the calculated compounds oxirane and thiirane at the B3LYP/6-311G(d) level are collected in Table 2. As can be seen in Table 2, the agreement for both bond lengths and bond angles in the compounds between the B3LYP results and experimental values²³ is quite good, with the bond lengths and angles in

(22) (a) Grev, R. S.; Schaefer, H. F.; Gaspar, P. P. *J. Am. Chem. Soc.* **1991**, *113*, 5638. (b) Holthausen, M. C.; Koch, W.; Apeloig, Y. *J. Am. Chem. Soc.* **1999**, *121*, 2623.

(23) (a) Hirose, C. *Bull. Chem. Soc. Jpn.* **1974**, *47*, 1311. (b) Okiye, K.; Hirose, C.; Lister, D. G.; Sheridan, J. *Chem. Phys. Lett.* **1974**, *24*, 111.

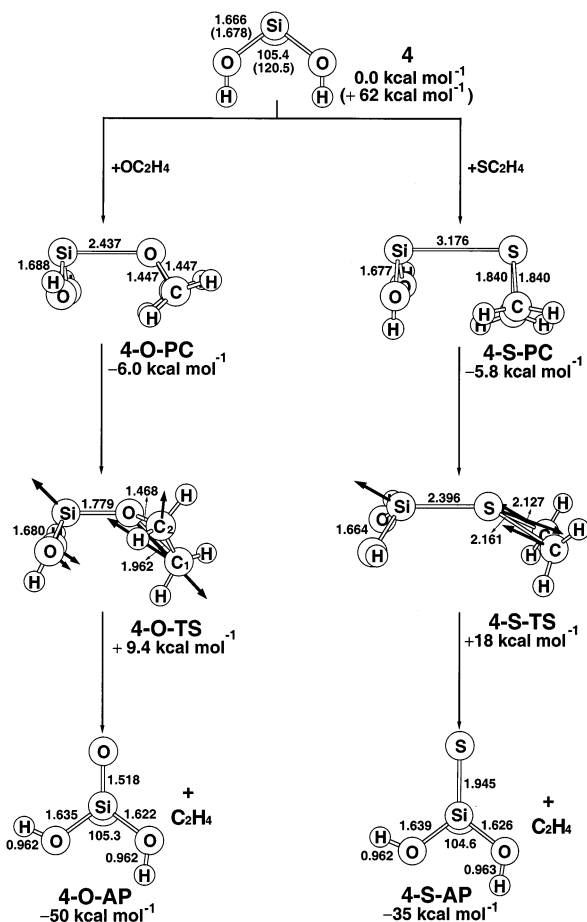


Figure 4. The B3LYP/6-311G(d) geometries (in Å and deg) for the precursor complexes (PC), transition states (TS), and abstraction products (AP) of oxirane with Si(OH)₂ (4). The relative energies were obtained at the QCISD level of theory. Values in parentheses are in the triplet state. The heavy arrows indicate the main atomic motions in the transition state eigenvector.

agreement to within 0.021 Å and 1.5°, respectively. It is, therefore, believed that the B3LYP calculations provide an adequate theoretical level for further investigations of molecular geometries, electronic structures, and kinetic features of the reactions.

Finally, it should be noted that, for all silylenes studied in this work, the excitation energies from the singlet ground state to the first triplet excited state are quite large (~19–72 kcal/mol). This means that production of the first excited triplet state under experimental conditions is practicably impossible. Thus, only the singlet potential surface was considered throughout this work.

B. Precursor Complexes. Let us now explore the potential energy surface for these abstraction reactions. It is reasonable to expect that the first step in the reaction of silylene with both oxirane and thiirane is the formation of a precursor complex (PC), which then decomposes through a four-center transition state (TS) to yield the eventual abstraction products (Pro). The optimized geometries and energies of the complexations of silylene with oxirane and thiirane, that is, 1-O-PC, 2-O-PC, 3-O-PC, 4-O-PC, 5-O-PC, 1-S-PC, 2-S-PC, 3-S-PC, 4-S-PC, and 5-S-PC, are shown in Figures 1–5, respectively. For convenience, the energies are given relative to those of the two reactant molecules, that is, SiX₂ + OC₂H₄ and SiX₂ + SC₂H₄, which are also summarized in Table 1.

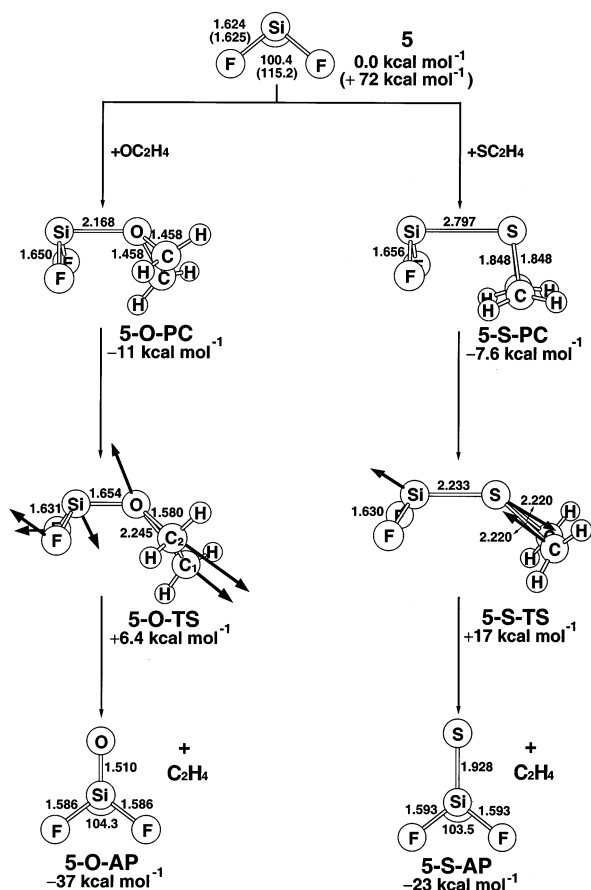


Figure 5. B3LYP/6-311G(d) geometries (in Å and deg) for the precursor complexes (PC), transition states (TS), and abstraction products (AP) of oxirane with SiF₂ (5). The relative energies were obtained at the QCISD level of theory. Values in parentheses are in the triplet state. The heavy arrows indicate the main atomic motions in the transition state eigenvector.

First, as seen in Figures 1–5, it is apparent that the precursor complexes all display very similar X₂Si---OC₂H₄ bonding characteristics in which the SiX₂ unit lies virtually parallel to the oxirane plane. Calculated vibrational frequencies for the precursor complexes reveal that these structures are true minima on the potential energy surfaces. In fact, these intermediates correspond to donor–acceptor complexes, stabilized by the interaction of lone pair electrons on the oxygen atom with a vacant *p*- π orbital on the silylene, as illustrated in Scheme 1. Indeed, from another point of view, these initial complexes can be considered as “ylide-like complexes”, since they all possess a similar ylide structure²⁴ with a long Si–O or Si–S bond.

When compared to the structures of the isolated reactants, both silylene and oxirane geometries in the precursor complexes are essentially unperturbed. Moreover, as one can see from Figures 1–5, the calculated bond distances for the Si---O contacts (~3.0–2.1 Å) are considerably longer than those calculated for the corresponding products (~roughly 1.5 Å; vide infra). Such large bond lengths are also reflected in the calculated complexation energies. Namely, the longer the Si–O distance, the smaller the binding energy of the precursor complex. For instance, our DFT results predict that the Si–O distances increase in the order: 1-O-PC (~2.1 Å) < 5-O-PC (~2.2 Å) \approx 2-O-PC (~2.2 Å) < 4-O-PC (~2.4 Å) < 3-O-PC

(24) Johnson, A. W. *Ylide Chemistry*; Academic Press: New York, 1966; p 251.

Table 1. Relative Energies for Singlet and Triplet Silylenes and for the Process Silylene + Oxirane (or Thiirane) → Precursor Complex → Transition State → Abstraction Products^{a,b}

| | system | ΔE_s^c (kcal mol ⁻¹) | ΔE_{pc}^d (kcal mol ⁻¹) | ΔE^e (kcal mol ⁻¹) | ΔH^f (kcal mol ⁻¹) |
|---|-----------------------------------|---|---|---|---|
| | | | OC ₂ H ₄ | | |
| 1 | SiH ₂ | +18.72 (+20.52) | -14.08 (-16.13) | -2.229 (-6.565) | -60.68 (-57.32) |
| 2 | Si(CH ₃) ₂ | +25.10 (+26.46) | -9.133 (-9.265) | +0.8732 (-2.923) | -67.67 (-64.89) |
| 3 | Si(NH ₂) ₂ | +56.38 (+55.97) | -1.348 (-1.431) | +18.54 (+15.68) | -54.50 (-47.66) |
| 4 | Si(OH) ₂ | +62.02 (+64.63) | -6.048 (-5.178) | +9.399 (+8.068) | -50.37 (-43.06) |
| 5 | SiF ₂ | +71.81 (+74.80) | -10.85 (-13.25) | +6.432 (+5.161) | -37.34 (-31.58) |
| | | | SC ₂ H ₄ | | |
| 1 | SiH ₂ | +18.72 (+20.52) | -16.80 (-17.41) | -4.895 (-10.84) | -46.71 (-46.89) |
| 2 | Si(CH ₃) ₂ | +25.10 (+26.46) | -9.929 (-7.991) | -1.755 (-4.391) | -52.65 (-52.04) |
| 3 | Si(NH ₂) ₂ | +56.38 (+55.97) | -1.390 (-0.7950) | +20.03 (+14.87) | -38.94 (-36.21) |
| 4 | Si(OH) ₂ | +62.02 (+64.63) | -5.778 (-5.340) | +17.60 (+13.61) | -34.69 (-31.76) |
| 5 | SiF ₂ | +71.81 (+74.80) | -7.646 (-9.452) | +16.88 (+10.11) | -22.84 (-21.06) |

^a At the QCISD and B3LYP (in parentheses) levels of theory. For the B3LYP optimized structures of the stationary points, see Figures 1–5. ^b Energies differences have been zero-point corrected. See the text. ^c Energy relative to the corresponding singlet state. A positive value means the singlet is the ground state. ^d The stabilization energy of the precursor complex relative to the corresponding reactants. ^e The activation energy of the transition state relative to the corresponding reactants. ^f The exothermicity of the product relative to the corresponding reactants.

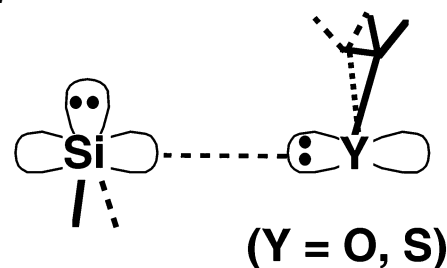
Table 2. Comparison of Structures of Oxirane and Thiirane^{a,b,c}

| | O | S |
|--------------|------------------|------------------|
| r(CY) | 1.429 (1.428) | 1.836 (1.815) |
| r(CC) | 1.467 (1.469) | 1.479 (1.484) |
| r(CH) | 1.088 (1.086) | 1.084 (1.083) |
| ∠CYC | 61.76 (61.62) | 47.47 (47.51) |
| ∠HCH | 115.4 (116.9) | 114.8 (114.5) |

^a At the B3LYP/6-311G(d) level. ^b Values in parentheses denote the experimental data. For oxirane (Y = O) and thiirane (Y = S), see ref 23 parts a and b, respectively. ^c Bond lengths are in Å, and bond angles are in degrees.

(~3.0 Å). The binding energies relative to those of their corresponding reactants follow a similar trend namely: 1-O-PC (-14 kcal/mol) < 5-O-PC (-11 kcal/mol) < 2-O-PC (-9.1 kcal/mol) < 4-O-PC (-6.0 kcal/mol) < 3-O-PC (-1.3 kcal/mol). It should be emphasized that the energies of these precursor complexes relative to their corresponding reactants are less than 14 kcal/mol. It, thus, appears unlikely that the silylene–oxirane complexes can be isolated experimentally at room temperature because their stabilization energies are too low.

Likewise, the ylide-like precursor complexes (1-S-PC, 2-S-PC, 3-S-PC, 4-S-PC, and 5-S-PC) for thiirane desulfuriza-

Scheme 1

tion were also located at the DFT level. Again, these adducts were confirmed to have no imaginary frequencies, indicating they are true minima on the potential energy surfaces. As mentioned above, these intermediates correspond to donor–acceptor complexes, stabilized by the donative interaction between lone pair electrons on the sulfur atom and a vacant *p*- π orbital on the silylene, as illustrated in Scheme 1. As shown in Figures 1–5, the Si–S distances in the precursor complexes decrease in the order: 3-S-PC (~3.8 Å) > 4-S-PC (~3.2 Å) > 5-S-PC (~2.8 Å) > 2-S-PC (~2.5 Å) > 1-S-PC (~2.4 Å). Again, such large bond distances are accompanied by small values for the complex stabilization energy. Indeed, the complexation energies relative to those of their corresponding reactants follow the same trend as the Si–S bond distances described above: 3-S-PC (-1.4 kcal/mol) > 4-S-PC (-5.8 kcal/mol) > 5-S-PC (-7.6 kcal/mol) > 2-S-PC (-9.9 kcal/mol) > 1-S-PC (-17 kcal/mol). Furthermore, of these five precursor complexes, 1-S-PC is the most stable, being calculated as 17 kcal/mol lower in energy than those of the corresponding reactants. However, its activation energy (relative to that of its corresponding precursor complex) is only 6.0 kcal/mol at the QCISD level of theory. According to these theoretical results, it is, therefore, predicted that the experimental observations of these silylene–thiirane complexes formed during the reactions will be difficult, since the interaction between the substituted silylene and thiirane is very weak.

C. Transition States. The optimized transition state structures (1-O-TS, 2-O-TS, 3-O-TS, 4-O-TS, 5-O-TS, 1-S-TS, 2-S-TS, 3-S-TS, 4-S-TS, and 5-S-TS) along with the calculated transition vectors are shown in Figures 1–5, respectively. The arrows in the figures indicate the directions in which the atoms move in the normal coordinate corresponding to the imaginary frequency. Examination of the single imaginary frequency for each transition state (389i cm⁻¹, 1-O-TS; 467i cm⁻¹, 2-O-TS; 445i cm⁻¹, 3-O-TS; 319i cm⁻¹, 4-O-TS; 186i cm⁻¹, 5-O-TS; 391i cm⁻¹, 1-S-TS; 296i cm⁻¹, 2-S-TS; 405i cm⁻¹, 3-S-TS; 404i cm⁻¹, 4-S-TS; and 375i cm⁻¹, 5-S-TS) confirms the concept of an abstraction process. That is to say, the vibrational motion during the deoxygenation of oxirane by silylene involves the bond forming between silicon and oxygen in concert with two O–C bonds breaking in the oxirane ring. A similar four-center pattern for the transition states can be found in the thiirane desulfurization as well. Apparently, these transition states connect the corresponding precursor complexes to the abstraction products.

One of the interesting points to emerge from calculations of TS geometries is the extent to which Si–O and Si–S bonds are formed in the transition state. The Si–O and Si–S bond lengths in the transition states of SiH₂, Si(CH₃)₂, Si(NH₂)₂, Si(OH)₂, and SiF₂ species are (13%, 10%), (14%, 11%), (40%,

35%), (27%, 25%), and (24%, 20%) shorter than those in the corresponding precursor complexes, respectively. All these features indicate that the SiH_2 and $\text{Si}(\text{CH}_3)_2$ abstraction reactions arrive at the TS relatively early, whereas the $\text{Si}(\text{NH}_2)_2$, $\text{Si}(\text{OH})_2$, and SiF_2 abstraction reactions reach the TS relatively late. According to the Hammond postulate,²⁵ the former silylenes should have lower activation barriers, and the latter, higher. This was fully confirmed by our theoretical calculations. As shown in Table 1, the barrier heights (QCISD) for the abstraction reactions increase in the order: 1-O-TS (-2.2 kcal/mol) < 2-O-TS (0.87 kcal/mol) < 5-O-TS (6.4 kcal/mol) < 4-O-TS (9.4 kcal/mol) < 5-O-TS (18 kcal/mol) and 1-S-TS (-4.9 kcal/mol) < 2-S-TS (-1.8 kcal/mol) < 5-S-TS (17 kcal/mol) < 4-S-TS (18 kcal/mol) < 5-S-TS (20 kcal/mol). In other words, the lower the electronegativity of the substituent, the earlier the transition state is formed, and the lower the barrier to abstraction.

Furthermore, the most dramatic result in our B3LYP calculations is that all the transition states for the oxygen transfer reactions are asynchronous, while for the thiirane desulfurization they are synchronous. For instance, as one can see in Figures 1–5, in the deoxygenation reaction, one of the breaking bonds ($\text{O}-\text{C}_1$) is greatly stretched (i.e., 1-O-TS, 1.89 Å; 2-O-TS, 1.79 Å; 3-O-TS, 1.86 Å; 4-O-TS, 1.96 Å; and 5-O-TS, 2.25 Å), whereas the other ($\text{O}-\text{C}_2$) is only slightly longer than a normal $\text{O}-\text{C}$ single bond in oxirane (i.e., 1-O-TS, 1.44 Å; 2-O-TS, 1.43 Å; 3-O-TS, 1.46 Å; 4-O-TS, 1.47 Å; and 5-O-TS, 1.58 Å). On the other hand, in the case of desulfurization, the two breaking $\text{S}-\text{C}$ bonds are almost equally stretched in the transition structures of SiH_2 (1-S-TS), $\text{Si}(\text{CH}_3)_2$ (2-S-TS), $\text{Si}(\text{NH}_2)_2$ (3-S-TS), $\text{Si}(\text{OH})_2$ (4-S-TS), and SiF_2 (5-S-TS). Regardless of whether these transition structures are formed synchronously or asynchronously, the present calculations indicate that both oxirane deoxygenation and thiirane desulfurization are still concerted, since no energy minimum corresponding to an intermediate between the transition state and the products has been found. Accordingly, our theoretical investigations suggest that both oxirane deoxygenation and thiirane desulfurization by silylene species should take place with complete retention of stereochemical integrity in the alkene. As there are no relevant experimental and theoretical data on such systems, the above result is a prediction.

D. Abstraction Products. The optimized product structures (1-O-AP, 2-O-AP, 3-O-AP, 4-O-AP, 5-O-AP, 1-S-AP, 2-S-AP, 3-S-AP, 4-S-AP, and 5-S-AP) are collected in Figures 1–5. To simplify comparisons and to emphasize the trends, the calculated reaction enthalpies for abstraction are also summarized in Table 1.

From Table 1, it is apparent that both oxirane deoxygenation and thiirane desulfurization by silylenes are exothermic and the order of exothermicity follows a similar trend to that of the activation energy. For example, the reaction enthalpies for oxirane deoxygenation increase in the order: $\text{Si}(\text{CH}_3)_2$ (2) (-68 kcal/mol) < SiH_2 (1) (-61 kcal/mol) < $\text{Si}(\text{NH}_2)_2$ (3) (-54 kcal/mol) < $\text{Si}(\text{OH})_2$ (4) (-50 kcal/mol) < SiF_2 (5) (-37 kcal/mol). Similarly, for thiirane desulfurization the reaction enthalpy increases in the order: $\text{Si}(\text{CH}_3)_2$ (2) (-53 kcal/mol) < SiH_2 (1) (-47 kcal/mol) < $\text{Si}(\text{NH}_2)_2$ (3) (-39 kcal/mol) < $\text{Si}(\text{OH})_2$ (4) (-35 kcal/mol) < SiF_2 (5) (-23 kcal/mol). Two intriguing points follow readily from the above. First, our computational

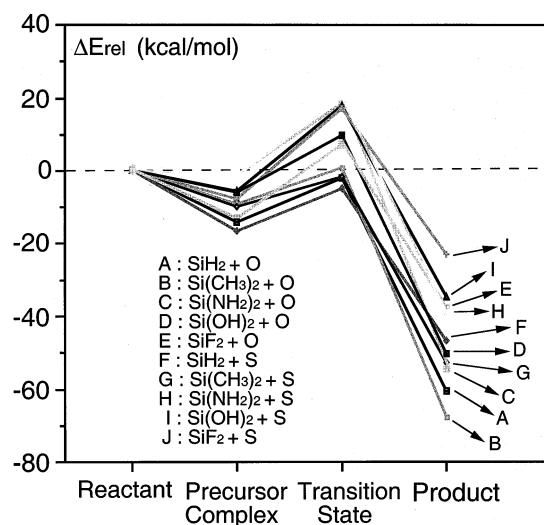


Figure 6. Potential energy surfaces for substituted silylenes toward the abstraction reactions with oxirane (O) and thiirane (S). The relative energies are taken from the QCISD level as given in Table 1. For the B3LYP optimized structures of the stationary points, see Figures 1–5.

results suggest that the reaction enthalpy of oxirane deoxygenation should be more exothermic than that of thiirane desulfurization. Second, for the substituted silylene species, a less electronegative as well as a more bulky substituent should lead to a more exothermic abstraction reaction.

E. Overview of Silylene Abstraction. A schematic diagram of the $\text{SiX}_2 + \text{OC}_2\text{H}_4$ and $\text{SiX}_2 + \text{SC}_2\text{H}_4$ ($\text{SiX}_2 = \text{SiH}_2$, $\text{Si}(\text{CH}_3)_2$, $\text{Si}(\text{NH}_2)_2$, $\text{Si}(\text{OH})_2$, and SiF_2) potential surfaces is displayed in Figure 6.

The major conclusions that can be drawn from Figure 6 and Table 1 are as follows:

(5) For both oxirane and thiirane systems, a precursor complex for the silylene abstraction reaction may not exist.

(6) The magnitudes of the silylene abstraction barriers are not high. This strongly implies that both deoxygenation and desulfurization should be facile processes at room temperature.

(7) For a given silylene species, the activation barrier for the oxirane deoxygenation is smaller than that for the thiirane desulfurization, indicating that the former is kinetically more favorable than the latter. In other words, providing reaction conditions remain the same, oxirane is more susceptible to a silylene abstraction reaction than thiirane.

(8) Abstraction of oxygen (or sulfur) from oxirane (or thiirane) by a singlet silylene should produce a silanonyl (or silanethionyl) compound and ethylene in a single step (i.e., in a concerted manner), thus, stereospecifically. Namely, such silylene abstractions should be favored for producing stereo-retention products.

(9) As discussed earlier, oxirane undergoes concerted deoxygenation by reaction with silylenes via an asynchronous transition state. In contrast, thiirane desulfurization reactions are predicted to be concerted but more synchronous, that is, via a transition structure with two more-or-less equally-breaking bonds.

(10) Using identical reaction conditions, the oxirane deoxygenation should be more exothermic than the thiirane desulfurization. Consequently, the production of silanonyl compounds (i.e., $>\text{Si}=\text{O}$) is clearly more thermodynamically favored than silanethionyl molecules (i.e., $>\text{Si}=\text{S}$).

(25) Hammond, G. S. *J. Am. Chem. Soc.* **1955**, *77*, 334.

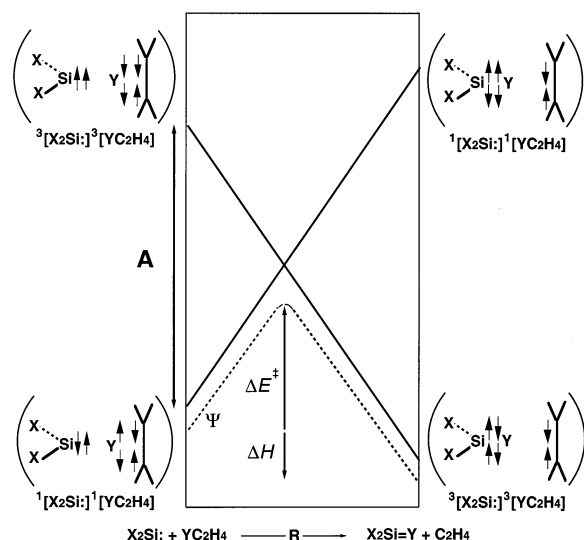


Figure 7. Energy diagram for an abstraction reaction showing the formation of a potential energy curve (Ψ) by mixing two configurations: the reactant configuration and the product configuration. In the reactants, they are separated by an energy gap A. Configuration mixing near the crossing point causes an avoided crossing (dotted line).

(11) Regardless of whether oxirane deoxygenation or thiirane desulfurization is considered, alkyl-substituted silylene abstractions are much more favorable than those of π -donor-substituted silylenes. That is to say, the less electronegative the substituent, the lower the activation barrier, and the more exothermic is the silylene abstraction.

(12) Electronic as well as steric factors should play an important role in determining the chemical reactivities of the silylene species from both a kinetic and thermodynamic viewpoint.

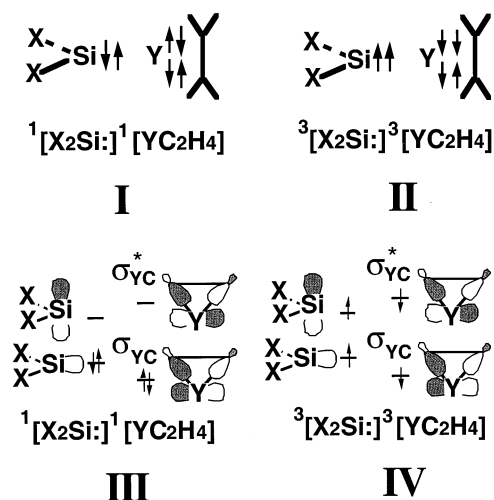
In short, considering both the activation barrier and exothermicity based on the model calculations presented here, we conclude that the silylenic reactivity order is as follows: $\text{SiH}_2 > \text{Si}(\text{CH}_3)_2 > \text{Si}(\text{NH}_2)_2 \approx \text{Si}(\text{OH})_2 \approx \text{SiF}_2$. In other words, electron-donating groups (or electropositive substituents) on the silylene accelerate the abstraction reaction, whereas electron-withdrawing groups (or π -donor substituents) on the silylene retard the reaction.

IV. Configuration Mixing Model

According to our theoretical analysis, all our computational results can be rationalized on the basis of a configuration mixing (CM) model which was developed by Pross and Shaik.^{26,27} In this section, we show how concepts deduced from the CM model can be used to predict the relative reactivities of the reactants.

Although, in principle, many electron configurations of the species involved in the abstraction reaction contribute to the precise form of the energy surface,^{26,27} there are only two predominant configurations that contribute significantly to the total wave function Ψ and, in turn, to the potential energy surface; see Figure 7. One is the reactant ground-state configuration that ends up as an excited configuration in the product region. The other is the excited configuration of the reactants that correlates with the ground state of the products.

The key valence bond (VB) configurations for the heteroatom transfer reaction are illustrated in I and II, while the key molecular orbital (MO) configurations are illustrated in III and IV.^{26,27} The VB configuration I, labeled $^1[\text{X}_2\text{Si:}]^1[\text{YC}_2\text{H}_4]$, is



termed the *reactant configuration* because this configuration is a good descriptor of the reactants; the two electrons on the $\text{X}_2\text{Si:}$ moiety are spin paired to form the lone pair, while the two electrons on the Y heteroatom are spin paired with the ethylene moiety to form two $\text{Y}-\text{C}$ σ bonds. On the other hand, configuration II is the VB *product configuration*. It might initially appear strange that triplet pairs are incorporated into the description of a singlet silylene abstraction reaction. In reality, however, there is no actual spin change here because, despite the fact that $^3[\text{X}_2\text{Si:}]^3[\text{YC}_2\text{H}_4]$ appears to contain two triplet pairs, the overall spin state of $^3[\text{X}_2\text{Si:}]^3[\text{YC}_2\text{H}_4]$ remains a singlet. Moreover, it is a doubly excited configuration only in the reactant geometry. In terms of the product geometry, it is not an excited configuration at all, just the configuration that describes the ground-state abstraction products.²⁸ The MO representations of VB configurations I and II are shown in III and IV, respectively. A schematic energy plot of I and II (or III and IV) for a heteroatom transfer reaction as a function of the reaction coordinate (the approach of a silylene to the YC_2H_4 molecule) is illustrated in Figure 7. The ground-state reaction profile, obtained by the mixing of reactant and product configurations, is indicated by the dashed curve and exhibits an activation energy barrier. Thus, it is the avoided crossing of these two configurations that leads to the simplest description of the ground-state energy profiles for abstraction reactions of the silylene species.^{26,27}

On the basis of Figure 7 for barrier formation in silylene abstraction reactions, we are now in a position to provide an insight into the parameters that are likely to affect reactivity in this system. The energy of point II (left in Figure 7), the anchor point for $^3[\text{X}_2\text{Si:}]^3[\text{YC}_2\text{H}_4]$ in the reactant geometry, will be governed by the singlet–triplet energy gap for both the silylene and the oxirane (or thiirane). That is, $\Delta E_{\text{st}} (= E_{\text{triplet}} - E_{\text{singlet}}$ for $\text{X}_2\text{Si:}) + \Delta E_{\sigma\sigma^*} (= E_{\text{triplet}} - E_{\text{singlet}}$ for $\text{YC}_2\text{H}_4)$. In other words, the smaller the $\Delta E_{\text{st}} + \Delta E_{\sigma\sigma^*}$ value, the lower the activation barrier, and the larger the exothermicity.^{26,27} Bearing the above analysis (Figure 7) in mind, we shall explain the origin

(26) Shaik, S.; Schlegel, H. B.; Wolfe, S. *Theoretical Aspects of Physical Organic Chemistry*; Wiley: New York, 1992.

(27) Pross, A. *Theoretical and Physical Principles of Organic Reactivity*; Wiley: New York, 1995.

(28) Pross, A.; Moss, R. A. *Tetrahedron Lett.* **1990**, *31*, 4553.

of the observed trends as shown previously in the following discussion.

Why are the alkyl-substituted silylene much more favorable than the π donor-substituted silylenes toward the abstraction reactions with oxirane and thiirane?

The driving force for this can be traced to the singlet–triplet energy gap (ΔE_{st}) of the silylene. As analyzed above, if $\Delta E_{\sigma\sigma^*}$ is a constant, the smaller the ΔE_{st} of silylene, the lower the barrier height, and the larger the exothermicity, and, in turn, the faster the heteroatom transfer reaction. Indeed, our theoretical calculations confirm this prediction and suggest an increasing trend in ΔE_{st} : SiH_2 (19 kcal/mol) < $\text{Si}(\text{CH}_3)_2$ (25 kcal/mol) < $\text{Si}(\text{NH}_2)_2$ (56 kcal/mol) < $\text{Si}(\text{OH})_2$ (62 kcal/mol) < SiF_2 (72 kcal/mol). From Table 1, it is readily seen that this result agrees qualitatively with the trend in activation energy and enthalpy (ΔE^\ddagger , ΔH) for oxirane deoxygenation, which is SiH_2 (−2.2, −61), $\text{Si}(\text{CH}_3)_2$ (0.87, −68), $\text{Si}(\text{NH}_2)_2$ (18, −54), $\text{Si}(\text{OH})_2$ (9.4, −43), and SiF_2 (6.4, −37), kcal/mol, respectively. Likewise, the same phenomenon can also be found in thiirane desulfurization as follows: SiH_2 (−4.9, −47), $\text{Si}(\text{CH}_3)_2$ (−1.8, −53), $\text{Si}(\text{NH}_2)_2$ (20, −39), $\text{Si}(\text{OH})_2$ (18, −35), and SiF_2 (17, −23) kcal/mol, respectively.

V. Conclusion

With the above analysis in mind, we are confident in predicting that electron-donating or bulky substituents on the silylene will result in a smaller ΔE_{st} and, in turn, will facilitate the heteroatom transfer reaction. On the other hand, it is anticipated that a silylene species with π -donor or electron-withdrawing substituents would lead to a larger ΔE_{st} . As a result, its reactivity toward the abstraction reaction would decrease. It should be emphasized that while both deoxygenation and

desulfurization are facile processes, the deoxygenation reaction is more exothermic as well as more kinetically favorable. Besides these, the present model calculations demonstrate that a concerted process, which does not involve ylide intermediates, should play a key role in such abstraction reactions. That is to say, these heteroatom transfer reactions by silylenes will proceed stereospecifically, leading to an olefin with retained stereochemistry.

Furthermore, as our analysis demonstrates, the CM approach adds additional facets and insights into this relatively poorly understood area of mechanistic study. Although the relative reactivities of various silylenes are determined by the entire potential energy surface, the concepts of the CM model, focusing on the singlet–triplet splitting in the reactants, allows one to assess quickly the relative reactivities of a variety of silylenes without specific knowledge of the actual energies of the interactions involved. Despite its simplicity, our approach can provide chemists with important insights into the factors controlling the activation energies for heteroatom transfer reactions and, thus, permit them to predict the reactivities of some unknown silylenes. The predictions may be useful as a guide to future synthetic efforts and to problems that merit further study by both theory and experiment.

We eagerly await experimental results to confirm our predictions.

Acknowledgment. The author is grateful to the National Center for High-Performance Computing of Taiwan for generous amounts of computing time. He also thanks the National Science Council of Taiwan for financial support.

JA020515L